

AN EDDY CURRENT METHOD FOR FLAW CHARACTERIZATION FROM
SPATIALLY PERIODIC CURRENT SHEETS

Satish M. Nair and James H. Rose

Center for NDE
Iowa State University
Ames, Iowa 50011

INTRODUCTION

Early NDE research primarily focused on the ability to develop techniques which could detect flaws in structures. Eddy currents, induced by exciting coil probes placed over a structure, were found to be a valuable tool in detecting flaws in conducting materials. In recent years, efforts have been expanded from the detection of defects to a more quantitative characterization of flaws. In metallic structures, the important flaw characteristics consist of the flaw's depth, position, size, shape, and material properties (flaw electrical conductivity, magnetic permeability etc.). This paper continues our efforts of the past two years to recover flaw characteristics from eddy current data.

The change in impedance due to an inclusion, surface breaking or buried, within a conducting halfspace is taken as the eddy current data. The inclusion is assumed to differ slightly in conductivity from the host material. Last year, a multi-frequency inverse method to obtain the flaw electrical conductivity was developed for the case of a uniform magnetic field applied on the surface [1,2]. The inversion kernel was found to be described by an inverse Laplace transform. Numerical codes, based on the singular value decomposition technique, were developed to invert the Laplace transform and thus the eddy current data. The uniformity in the applied field however restricts the amount of information that can be extracted about the flaw; namely, one can only determine its conductivity as a function of depth. To recover the conductivity variation in the other directions, a spatially non-uniform field needs to be applied on the metal surface.

In this paper, we describe a multi-frequency method to recover the entire 3-D conductivity profile of the flaw (for small conductivity variations). A time-harmonic spatially periodic current sheet is placed over the metal surface and the resulting impedance changes due to the flaw are taken to be the data. For practical purposes, field distributions of this nature may be generated by a set of meander coils lying on the metal surface. The proximity of two adjacent current

carrying wires will determine the applied spatial frequency. Periodic variations are chosen since they allow us to analyze an arbitrary current coil distribution in terms of its spatial Fourier components. Consequently, inversion methods for various coil configurations can be synthesized from the results presented in the paper.

This paper is structured in the following manner. We start with the volume integral form of expression for the impedance change due to an inclusion, differing in conductivity alone, within a metallic halfspace [3,4]. The linearized form of this expression is taken to derive the impedance change for a spatially periodic current sheet placed over the metal's surface. The impedance change is seen to be a function of both the spatial and harmonic frequencies through a coupled Fourier-Laplace transform. It is not clear how this coupled transform can be inverted in the harmonic frequency domain. The time domain version of the impedance change is then derived. It is seen that the transform variables decouple. Hence, an explicit inversion algorithm can be written down. Finally, we describe this inversion procedure and the steps required to extract the 3D conductivity variation within the halfspace.

IMPEDANCE CHANGE FOR A SPATIALLY PERIODIC CURRENT SHEET - FREQUENCY DOMAIN

Consider a 3D inclusion in a conducting halfspace, with a conductivity slightly different from the host. A spatially periodic current sheet of either cosine or sinusoidal spatial dependence is placed over the conductor, perpendicular to the direction of spatial variation. See Figure 1. The applied spatial frequency is denoted by q . For such an example, the impedance change due to the inclusion is given in [4] as

$$\delta z = -\frac{1}{I^2} \int_{V_{\text{hsp}}} \delta \sigma (\underline{E} \cdot \underline{E}') dV. \quad (1)$$

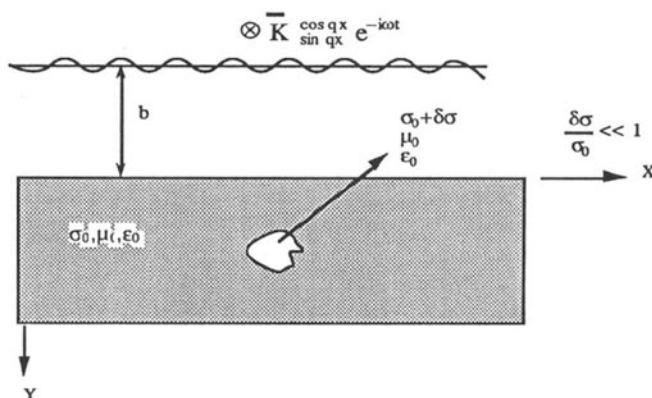


Fig. 1. Inclusion in a metallic halfspace under an applied spatially periodic current sheet

For a "weakly conductive inclusion", we linearize the above equation (the Born approximation). The electric field, \underline{E}' , is therefore approximated by \underline{E} , the electric field in the absence of the flaw. \underline{E} can be computed by solving Maxwell's laws for a spatially periodic current sheet over a homogeneous conducting halfspace and is given by

$$\underline{E}|_{\cos qx} = \frac{k_0^2}{\sigma_0} \bar{K} \frac{e^{-qb} e^{iky}}{q-ik} \cos qx \hat{z} \quad (2a)$$

$$\underline{E}|_{\sin qx} = \frac{k_0^2}{\sigma_0} \bar{K} \frac{e^{-qb} e^{iky}}{q-ik} \sin qx \hat{z}, \quad (2b)$$

where

$$k = (k_0^2 - q^2)^{1/2}; k_0^2 = i\omega\mu_0\sigma_0; \text{Im}(k) > 0.$$

These results are computed in the quasistatic approximation and details can be found in Stoll [5]. Substituting Eqs. 2(a) and (b) in (1), we have the impedance change for a cosine and sinusoidal applied field given by

$$\delta z|_{\cos qx} \approx -\frac{\bar{K}^2 k_0^4}{I^2 \sigma_0^2 (q-ik)^2} \int_{V_{\text{hsp}}} dV \delta\sigma(\underline{x}) e^{2iky} \cos^2 qx \quad (3a)$$

$$\delta z|_{\sin qx} \approx -\frac{\bar{K}^2 k_0^4}{I^2 \sigma_0^2 (q-ik)^2} \int_{V_{\text{hsp}}} dV \delta\sigma(\underline{x}) e^{2iky} \sin^2 qx \quad (3b)$$

Define $\delta z|_{c-s}$ as the difference in impedance changes between a cosine and sinusoidal applied field at a fixed spatial frequency i.e.

$$\delta z|_{c-s} \equiv \delta z|_{\cos qx} - \delta z|_{\sin qx}. \quad (4)$$

Using results from Eq. 3(a) and (b), we have

$$\int_{V_{\text{hsp}}} dV \delta\sigma(\underline{x}) e^{2iky} \cos 2qx \approx -\delta z|_{c-s} \left[\frac{\bar{K}^2}{I^2} \frac{(q+ik)^2 e^{-2qb}}{\sigma_0^2} \right]^{-1}. \quad (5)$$

Generally, the impedance change can be measured for various spatial (q) and harmonic (ω) frequencies. Our problem is to recover $\delta\sigma(\underline{x})$ from the impedance $\delta z|_{c-s}$. Eq. (5) shows that such a recovery is possible if we can invert the coupled Fourier-Laplace transform. The coupling arises from the fact that k is a complex function of both q and ω .

Consider the inversion of this coupled Fourier-Laplace transform. Assume that the impedance changes are given for all real spatial and harmonic frequencies. The inversion over k is described by a complex Laplace transform. For a fixed q , varying ω implies tracing hyperbolas described by

$$[\text{Im}(k)]^2 - [\text{Re}(k)]^2 = q^2 \quad (6)$$

where

$$2 \operatorname{Re}(k) \operatorname{Im}(k) = \omega \mu_0 \sigma_0. \quad (7)$$

Data given for all real values of ω and q imply that data is known along these hyperbolas in the complex k plane, as shown in Figure 2. At $q = 0$, the hyperbola takes the form of a 45° line through the origin. This arises when the applied field is uniform over the surface.

The recovery of $\delta\sigma(\underline{x})$ therefore consists of inverting the complex Laplace transform over k when data is known only along these hyperbolas in the complex k -plane. Generally, methods to invert complex Laplace transforms require the knowledge of data over the entire complex plane. Recently, the authors have developed a technique to invert complex Laplace transforms when the data is known along any straight line through the origin in the complex plane [6]. This can be used to invert the data for the $q=0$ case. But for arbitrary q 's, when the data is known along the above-described hyperbolas, it is unclear how the complex Laplace transform can be inverted. It therefore appears that the spatial and harmonic frequency terms must somehow be decoupled, if an explicit inversion algorithm to recover the conductivity characteristic function $\delta\sigma(\underline{x})$ from the impedance δz is to be written down.

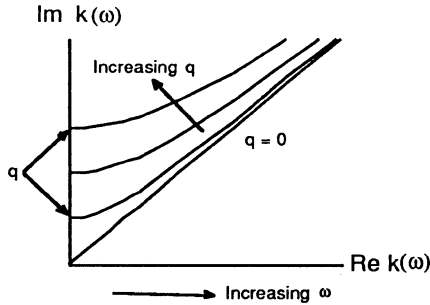


Fig. 2. Hyperbolic curves in the complex k -plane along which impedance data are typically known.

IMPEDANCE CHANGE FOR A SPATIALLY PERIODIC CURRENT SHEET - TIME DOMAIN

It was seen in the previous section that the impedance change in the frequency domain is given by a coupled Fourier-Laplace transform of the conductivity characteristic function $\delta\sigma(\underline{x})$. This coupling poses a problem in inverting the transforms to extract $\delta\sigma(\underline{x})$. In developing an inversion method for a uniformly applied field [2], it was seen that the inversion kernel is complex in the frequency-domain whereas it is real in the time-domain. This proved to be extremely useful in numerically implementing the inverse expression in the time-domain.

Similarly, we shall study the behavior of the impedance change in the time-domain for an applied spatially periodic current sheet. This is obtained by taking inverse Fourier transforms of Eq. 5 with respect to the harmonic frequency, ω , i.e.

$$F^{-1} \left[\frac{\delta z|_{c-s}}{(q+ik)^2} \right] = -\frac{K^2 e^{-2qb}}{I^2 \sigma_0^2} F^{-1} \left[\int_{V_{imp}} dV \delta\sigma(x) e^{2iky} \cos 2qx \right]. \quad (8)$$

k is the only variable which depends on ω in the integrand on the right-hand side of the equation. The inverse Fourier transform of e^{2iky} therefore needs to be evaluated. Making a transformation of variables from ω to k^2 , we have

$$\frac{1}{2\pi} \int_{-\infty}^{\infty} e^{2iky} e^{-i\omega x} d\omega = \frac{1}{2\pi} \int_{-q}^{-q+i\infty} e^{2iky} e^{-\left(\frac{k^2+q^2}{\mu_0\sigma_0}\right)} \frac{d(k^2)}{i\mu_0\sigma_0}. \quad (9)$$

The integration contour in the k^2 plane is described in Figure 3. Since the integrand is multivalued, the branch of k in e^{2iky} needs to be specified. However, we have restricted $\text{Im}(k) > 0$ (in Eqs. 2 (a) and (b), the fields are assumed to vanish at infinity). Further, we assume that the time-domain impedance is causal. This implies that the impedance at negative frequencies is given by the complex conjugate of the impedance at positive frequencies,

$$\delta z(-|\omega|) = \delta z^*(|\omega|). \quad (10)$$

The above two conditions determine the choice of the branch for k and the appropriate branchcut is given by the positive real axis of the k^2 plane. See Figure 3. Using Eq. 10, Eq. 9 can be reduced to an integration in the upper-half k^2 plane given by

$$\frac{1}{2\pi} \int_{-\infty}^{\infty} e^{2iky} e^{-i\omega x} d\omega = \frac{1}{\pi i \mu_0 \sigma_0} e^{-\frac{q^2 x}{\mu_0 \sigma_0}} \text{Im} \int_{-q}^{-q+i\infty} e^{2iky} e^{-\frac{k^2 x}{\mu_0 \sigma_0}} d(k^2). \quad (11)$$

Note that $k(-|\omega|) = -k^*(|\omega|)$. The integration contour is now represented by Γ_1 in Figure 4. Since the integrand is analytic everywhere in the quadrant $\text{Im}(k^2) > 0$, $\text{Re}(k^2) < 0$, we have from Cauchy's theorem

$$\oint_{\Gamma_0 + \Gamma_1 + \Gamma_2 + \Gamma_{\infty}} e^{2iky} e^{-\frac{k^2 x}{\mu_0 \sigma_0}} d(k^2) = 0. \quad (12)$$

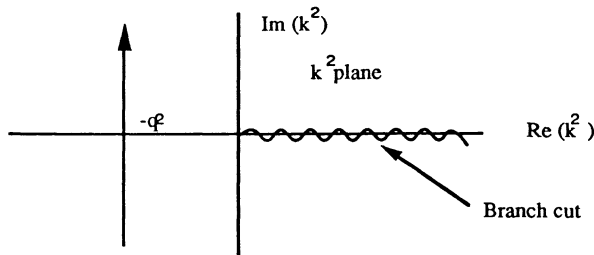


Fig. 3. Integration contour for the inverse Fourier transform described by Eq. (9).

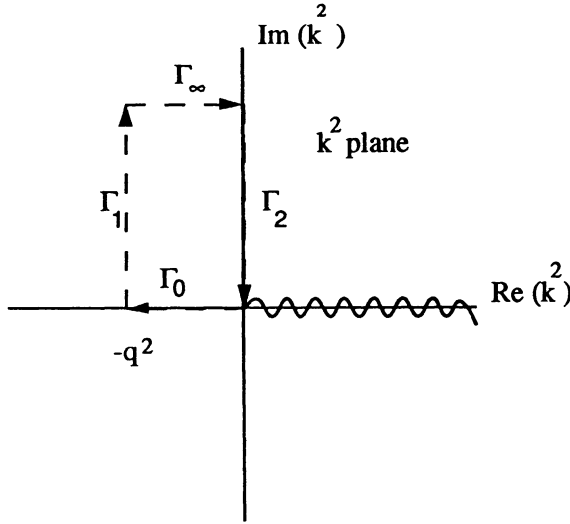


Fig. 4. Integration contour in the upper-half k^2 plane described by Eq. (11)

Consider the integrals over each of these contours individually.

$$1. \int_{\Gamma_{\infty}} e^{2iky} e^{-\frac{k^2 t}{\mu_0 \sigma_0}} d(k^2) = \lim_{R^2 \rightarrow \infty} \int_{-q^2 + iR^2}^{0 + iR^2} e^{2iky} e^{-\frac{k^2 t}{\mu_0 \sigma_0}} d(k^2). \quad (13)$$

This can be rewritten as

$$\lim_{R^2 \rightarrow \infty} \int_{-q^2 + iR^2}^{0 + iR^2} e^{2iky} e^{-\frac{k^2 t}{\mu_0 \sigma_0}} d(k^2) = \lim_{R^2 \rightarrow \infty} \int_{-q^2}^0 e^{2i(k_R^2 + iR^2)^{1/2} y} e^{-\frac{k_R^2 t}{\mu_0 \sigma_0}} e^{-\frac{iR^2 t}{\mu_0 \sigma_0}} d(k_R^2) \quad (14)$$

Since $\text{Im}(k_R^2 + iR^2)^{1/2} > 0$ and $|k_R^2 + iR^2|^{1/2} = (k_R^4 + R^4)^{1/4}$,

$$\lim_{R^2 \rightarrow \infty} \int_{-q^2}^0 e^{2i(k_R^2 + iR^2)^{1/2} y} e^{-\frac{k_R^2 t}{\mu_0 \sigma_0}} e^{-\frac{iR^2 t}{\mu_0 \sigma_0}} d(k_R^2) \rightarrow 0 \text{ for all } y > 0. \quad (15)$$

$$2. \int_{\Gamma_0} e^{2iky} e^{-\frac{k^2 t}{\mu_0 \sigma_0}} d(k^2) = \int_0^{-q^2} e^{2iky} e^{-\frac{k^2 t}{\mu_0 \sigma_0}} d(k^2). \quad (16)$$

The argument of k on Γ_0 is equal to $\pi/2$. Eq. (16) can be written as

$$\int_{\Gamma_0} e^{2iky} e^{-\frac{k^2 t}{\mu_0 \sigma_0}} d(k^2) = \int_0^{-q^2} e^{-2y|k|} e^{-\frac{k^2 t}{\mu_0 \sigma_0}} d(k^2). \quad (17)$$

Since the integrand is purely real and the values of k^2 are real, we see that the result will also be purely real. However, as seen from Eq. (11), we are only interested in the imaginary part of the above integral. The integral along Γ_0 has no contribution to this imaginary part.

Consequently, we now have

$$\text{Im} \int_{\Gamma_1} e^{2iky} e^{-\frac{k^2 t}{\mu_0 \sigma_0}} d(k^2) = -\text{Im} \int_{\Gamma_2} e^{2iky} e^{-\frac{k^2 t}{\mu_0 \sigma_0}} d(k^2). \quad (18)$$

Along Γ_2 , $q = 0$ and the integral is identical to that evaluated for a uniform field [1]. The spatial periodicity seems to be in effect attenuating the time-domain impedance response by the factor $e^{-q^2 t / \mu_0 \sigma_0}$. The integral in Eq. (18) can be evaluated and is given as

$$-\text{Im} \int_{\Gamma_2} e^{2iky} e^{-\frac{k^2 t}{\mu_0 \sigma_0}} d(k^2) = \pi^{1/2} y \left(\frac{\mu_0 \sigma_0}{t} \right)^{3/2} e^{-\frac{y^2 \mu_0 \sigma_0}{t}}. \quad (19)$$

Using this result in Eq. (11) and then resubstituting in Eq. (8), we have the time-domain impedance response given by

$$F^{-1} \left[\frac{\delta z|_{c-s}}{(q+ik)^2} \right] = -\frac{\bar{K}^2 e^{-2qb} e^{-\frac{q^2 t}{\mu_0 \sigma_0}}}{I^2 \sigma_0^2} \left(\frac{\mu_0 \sigma_0}{\pi} \right)^{1/2} \int_{V_{\text{hsp}}} dV \delta\sigma(x) y e^{-\frac{y^2 \mu_0 \sigma_0}{t}} \cos 2qx. \quad (20)$$

If we make the substitution $c^2 = (\mu_0 \sigma_0 / 2)$, $s = 2c^2 / t$, and $u = y^2$, we can rewrite this as

$$F^{-1} \left[\frac{\delta z|_{c-s}}{(q+ik)^2} \right] = -\frac{\bar{K}^2 e^{-2qb} e^{-q^2 t / s}}{I^2 \sigma_0^2} \frac{e^{-q^2 t / s}}{4c^2 \pi^{1/2}} \int_{-\infty}^{\infty} \int_{-\infty}^{\infty} \int_{-\infty}^{\infty} dx du dz \delta\sigma(x, u, z) e^{-su} \cos 2qx. \quad (21)$$

Making use of the causality of the impedance response in the time-domain, as demonstrated by Eq. (10) and noting that the direction of spatial variation is arbitrary in the XZ plane, Eq. (21) can be rewritten as

$$\begin{aligned} & \int_{-\infty}^{\infty} \int_{-\infty}^{\infty} \int_{-\infty}^{\infty} dx du dz \delta\sigma(x, u, z) e^{-su} \cos 2q \cdot \underline{x} \\ &= -e^{2|q|b} s^{-3/2} e^{q^2 t / s} \text{Re} \int_0^{\infty} d\omega \frac{\hat{\delta z}(\omega, q_x, q_z)}{[|q| + i(2ic^2 \omega - |q|^2)^{1/2}]^2} e^{-\frac{i\omega 2c^2}{s}} \\ & \text{where } \hat{\delta z}(\omega, q_x, q_z) = \delta z(\omega, q_x, q_z) \left[\frac{\bar{K}^2 \pi^{1/2}}{I^2 \sigma_0^2 4c^2} \right]^{-1}. \end{aligned} \quad (22)$$

The time-domain impedance response (or alternately, the inverse Fourier transform of the impedance in the frequency domain) is now obtained by real Laplace and Fourier transforms of the conductivity characteristic function. The transform variables are also decoupled in this domain. Hence, an explicit inversion procedure can be written down to recover the conductivity characteristic function.

The inversion procedure, based on Eq. (22), will then consist of the following steps:

1. Compute the inverse frequency-domain Fourier transform of the impedance to convert to the time-domain.
2. Evaluate the inverse cosine transform over q . This will give us the x and z variations of the conductivity characteristic function.

3. Evaluate the inverse Laplace transform over s for each value of x and z . Numerical codes for these were developed last year to invert the impedance when a uniform field was applied on the surface. This inversion will give us the complete 3D variation of the conductivity characteristic function.

CONCLUSION

In summary, an eddy current inverse method to detect small conductivity variations in a metallic halfspace has been developed. The method is based on a spatially periodic field being applied on the surface. The inversion kernel is seen to be governed by a coupled Fourier-Laplace transform in the frequency domain; the coupling occurring between the spatial and harmonic frequency. One way to decouple these transforms is to go into the time-domain. An inversion procedure, based on a time-domain representation of the impedance, is described. Numerical implementation of the inversion is currently in progress.

ACKNOWLEDGEMENT

This work was supported by the Center for NDE at Iowa State University and was performed at the Ames Laboratory. Ames Laboratory is operated for the U. S. Department of Energy by Iowa State University under Contract No. W-7405-ENG-82.

REFERENCES

1. S. M. Nair, J. H. Rose, and V. G. Kogan, in Review of Progress in Quantitative NDE, edited by D. O. Thompson and D. E. Chimenti, (Plenum Press, New York, 1988), Vol. 7A, pp. 461-469.
2. S. M. Nair and J. H. Rose, in Review of Progress in Quantitative NDE, edited by D. O. Thompson and D. E. Chimenti, (Plenum Press, New York, 1989), Vol. 8A, pp. 313-320.
3. B. A. Auld, F. G. Muennemann, and M. Riazat, in Research Techniques in Nondestructive Testing, Vol. 7, edited by R. S. Sharpe (Academic Press, London, 1984), Ch. 2.
4. W. S. Dunbar, *J. of Nondestructive Evaluation*, Vol. 7, Nos. 1/2, 43(1988).
5. R. L. Stoll, The analysis of eddy currents (Clarendon Press, Oxford, 1974).
6. S. M. Nair and J. H. Rose, unpublished.